CHAPTER 5

A NON-LINEAR MODIFIED CONVEF-AD BASED APPROACH FOR LOW-DOSE SINOGRAM RESTORATION

This work focuses on an approach for statistical sinogram smoothing for low-dose CT reconstruction. The proposed method is modelled into a variational framework. The solution of the method, based on minimization of an energy functional, consists of two terms viz. data fidelity term and a regularization function. The data fidelity term is obtained by minimizing the negative log likelihood of the signal dependent Gaussian probability distribution, which depicts the noise distribution in low dose X-ray CT. The second term i.e. regularization term is a non-linear CONVEF-AD (CONvolutional Virtual Electric Field Anisotropic Diffusion) based filter, which is an extension of Perona–Malik (P–M) anisotropic diffusion filter. The role of regularization function is to resolve the ill-posedness of first term. The proposed method is capable of dealing with both signal dependent and signal independent Gaussian noise i.e. mixed noise. For experimental purpose, two different sinograms generated from test phantom images are used. The comparative study and performance evaluation of the proposed method with other standard methods is also presented. The obtained results indicate that the proposed method possess better mixed noise removal capability than other methods in low dose X-ray CT.

5.1 Introduction

X-ray computed tomography (CT) is one of the most widely used medical imaging modalities for various clinical applications such as diagnosis and image-guided interventions. Recent discoveries regarding the potential harmful effects of X-ray radiation including lifetime risk of genetic, cancerous and other diseases (Yu, Lifeng *et. al.,* 2015) have raised growing concerns to patients and medical physics community (Yu, Lifeng *et. al.,* 2015). Therefore, minimizing the radiation risks is strongly desirable in clinical practices. To realize this objective, numerous studies have focused on radiation dose reduction of CT examinations (Yu, Lifeng *et. al.,* 2015; Zhang H *et. al.,* 2014; Gao Yang *et. al.,* 2014; Whiting Bruce *et. al.,* 2014). According to the International Commission on Radiological Protection (ICRP), patient doses in CT, especially in case of children, should always be kept as ALARA principle: "*as low as reasonably achievable*", see ICRP (2007) (Yu, Lifeng *et. al.,* 2015).

In the past decade, two classes of strategies have been exploited extensively for radiation dose reduction: (1) reducing the X-ray tube current and shortening the exposure time (i.e., milli ampere-second (mAs)) or the X-ray tube voltage (i.e., kilo voltage (kV)) settings to reduce the X-ray photon flux towards at each projection view; and (2) reducing the number of projection views per rotation during projection data acquisition. (Gao Yang *et. al.,* 2014)

Reducing the X-ray tube current and shortening the exposure time around the body, would inevitably increase the noise in projection/sinogram data, and the resulting image by the conventional analytical filtered back-projection (FBP) method (Whiting Bruce *et. al.,* 2014) may be severely degraded due to excessive X-ray poisson noise (Zhang *et. al.,* 2010). The later strategy would produce under sampled projection/sinogram data, and the resulting images by the FBP method would suffer from view-aliasing artifacts due to insufficient angular sampling. Sometimes, these two strategies are even combined, leading to both noisy and under sampled sinogram data, and the corresponding image reconstructed by the FBP method can be further degraded. Many algorithms to implement these strategies have been proposed for radiation dose reduction of CT examinations (Yu, Lifeng *et. al.,* 2015; Zhang H *et. al.,* 2014; Gao Yang *et. al.,*

2014; Zhang *et. al.,* 2010; Liu Li *et. al.,* 2012; Cui Xueying *et. al.,* 2014). Among these algorithms, preprocessing the noisy sinogram smoothing by statistical iterative methods have shown great potential to reduce the radiation dose while maintaining the image quality in X-ray CT as compared with the FBP reconstruction algorithm.

In the previous literature (Yu, Lifeng *et. al.,* 2015; Zhang H *et. al.,* 2014; Gao Yang *et. al.,* 2014; Zhang *et. al.,* 2010; Liu Li *et. al.,* 2012; Cui Xueying *et. al.,* 2014), Poisson noise is incorporated due to the limited number of detected photons counts in low-dose x-ray CT plus other background electronic noise is considered due to the electronic fluctuation in detector photodiode and other components. The acquired projection data by low energy radiation were considered to follow a signal–dependent compound poisson distribution plus a signal–independent Gaussian or normal distribution with zero mean (Liu Li *et. al.,* 2012). After that, a penalized Poisson likelihood maximization algorithm was then proposed. Later, a compound Poisson distribution model (Cui Xueying *et. al.,* 2014) was proposed, which takes into account both the characteristics of the energy-integrating sensors in the X-ray CT detector and the energy spectrum of X-ray beam. Since then, previous works (Jing Wang *et. al.,* 2008; Chen Y *et. al.,* 2010) described the calibrated and log transformed projection data of low-dose CT approximately follow a Gaussian distribution. Afterwards, the penalized weighted least-squares (PWLS) approach (Jing Wang *et. al.,* 2008) was applied to the noisy sinogram, thus, the optimal estimation of the projection data was obtained for FBP reconstruction. Recently, a generalized Gibbs prior (Zhen Tian *et. al.,* 2011) was designed to exploit nonlocal information of the projection data for the noisy sinogram and used the FBP method to finish the final CT reconstruction. The Bayesian statistical reconstruction for low-dose X-ray CT using an adaptive weighting nonlocal prior has been studied in (Chen Y *et. al.,* 2010) and got satisfactory effects.

For the sinogram smoothing purpose, it is very important to consider a widely studied effective regularization terms or priors (Liu Li *et. al.,* 2012; Cui Xueying *et. al.,* 2014; Jing Wang *et. al.,* 2008; Chen Y *et. al.,* 2010). Lowering the noise effect and preserving the edges are the two main aims in devising priors. But one drawback of these priors is their tendency to uniformly penalize the image

or the image gradient irrespective of the underlying image structures and the difference of signal-dependent noise properties in different regions. As a result, edges are sometimes over smoothed, leading to loss of detailed information. To address this drawback, several priors including smoothing, edge-preserving regularization terms and iterative algorithms with varying degrees of success have been already studied to obtain high-quality CT reconstruction images from low-dose projection data (Cui Xueying *et. al.,* 2014; Jing Wang *et. al.,* 2008; Chen Y *et. al.,* 2010; Srivastava Rajeev *et. al.,* 2013).

In the following paragraph at first we present a brief review of various diffusion based priors applied in image denoising problems are presented. After this a discussion about the possibilities of applying modified CONVEF-based P–M approach for restoration of low dose sinogram data is carried out. It is found that the Laplace operator can be used for image smoothing (Yuanquan Wang *et. al.,* 2010; Huaibin Wang *et. al.,* 2012), and for this purpose heat diffusion Eq., an isotropic diffusion, can cause blurring of the edges (Yuanquan Wang *et. al.,* 2010). A selective smoothing method, which makes the computation of gradient more stable through the use of a Gaussian filter and can also remove the isolated noise spot, was proposed in (Huaibin Wang *et. al.,* 2012). However, it presented the problem of edge blur. This problem was resolved by introducing diffusion tensor to make the diffusion faster in one direction than in other (Huaibin Wang *et. al.,* 2012). Afterwards, a diffusion based on trace to eliminate the influence of the interference term and to avoid the seeking of the best difference method in calculations was presented (Zhang Hao *et. al.,* 2015). The total Variation (TV) denoising model (Niu Shanzhou *et. al.,* 2014) which was stable than the P–M Eq. (Srivastava Subodh *et. al.,* 2012) was presented. Thereafter, the denoising algorithm based on TV was studied and applied widely (Cui Xueying *et. al.,* 2014; Niu Shanzhou *et. al.,* 2014; Srivastava Subodh *et. al.,* 2012; Zhang *et. al.,* 2013; Zhen Tian *et. al.,* 2011). However, the TV-based approach caused staircase effect. A more effective solution to this shortcoming is to increase the order of the derivative. Further, the shock filters which is a combination of two terms inverse (shock) and forward diffusion processes to make the diffusion process faster and to open the new dimensions in the field of image enhancement and restoration was introduced (Ghita O *et. al.,* 2010).

Furthermore, an anisotropic diffusion nonlinear partial differential Eq. (PDE) based diffusion process (Perona and Malik, 1990) was developed as a typical feature-preserving denoising technique. In this process the diffusion is controlled by a variable coefficient in order to preserve edges. After that, the gradient vector flow (GVF) field (Hongchuan yu, 2004) was developed for the implementation of the anisotropic diffusion models. But it has the disadvantage to produce undesirable staircase effect around smooth edges. Due to this effect, this method could not remove the isolated noise accurately and falsely recognize the boundaries of different blocks that actually belong to the same smooth area as edges.

A variety of high order denoising techniques has been developed (Perona and Malik, 1990; Hongchuan yu, 2004; Yuanquan Wang, 2008; Zhang Quan *et. al.,* 2013; Gui Z.g, 2013) to overcome the staircase effect and to improve the ability of denoising. The fourth-order PDE (Huaibin Wang *et. al.,* 2012) for noise removal presented a representative for this group, seeks to approximate the noisy image with a piecewise harmonic one and overcomes the staircase effect effectively. In view of these problems, the second-order derivatives at the direction of level set and gradient in (Hongchuan yu, 2004) are acquired through direct calculation on the noisy image, so the denoising effect can be affected because of the low numerical stability. Furthermore, to minimize the denoising effects, the gradient vector flow (GVF) field was incorporated as an external force for active contour model (Yuanquan Wang, 2008), into the anisotropic diffusion. However, due to presence of mixed noise in the sinogram data i.e. signal dependent and signal independent Gaussian noise; these methods cannot be applied directly. Even, GVF fields have no ability to find edge when images are corrupted by extraneous or Gaussian noise, and thus the denoising effect of mixed noisy images remains unsatisfactory. Afterwards, a new modified GVF (INGVF) field was introduced (Ghita O *et. al.,* 2010) into the P–M Eq. in order to remove both signal dependent and signal independent Gaussian noise. But, both the models GVF and INGVF are computationally expensive because they have to iteratively solve the generalized diffusion equations on the whole image.

In this work, modified CONVEF-based P–M approach is used as a prior term to deal with the issues of low dose CT image reconstruction. The modified

CONVEF-AD Eq. is used for smoothing of mixed noise sinogram data affected. The modified CONVEF-AD serves as regularization or smoothing term for low dose sinogram restoration to deal with the problem of ill-posedness and possess better reconstruction result. The presented reconstruction model has many desirable properties, such as superior noise robustness, reduced computational cost, the improved denoising effect and better edge & structure preserving properties. It can also overcome the staircase effect effectively. The proposed model performs well in low dose X-ray CT image reconstruction. Besides some relevant works of classical diffusion models, the results are also compared with some recently developed non-diffusion based approaches (Ghita O *et. al.,* 2010; Perona and Malik, 1990; Hongchuan yu, 2004; Yuanquan Wang, 2008; Zhang Quan *et. al.,* 2013; Gui Z.g, 2013).

Rest of the work is divided into the following sections. Section 2 presents the methods and materials of the work. Section 3, describes the proposed variational framework for sinogram restoration using CONVEF-AD regularized statistical image reconstruction method. Section 4 presents results and discussion of the simulation experiments and verifies that best results can be achieved by CONVEF-AD reconstruction method in both the simulated data and CT data. The conclusion is given in Section 5.

5.2 Background work

Noise modelling of the projection (or sinogram) data, specifically for low-dose CT, is essential for the statistics-based sinogram restoration algorithms. Low-dose (or mAs) CT sinogram data were usually contained serious stair-case artifacts and follow a Gaussian distribution with a nonlinear signal de-pendent and signal independent noise between the sample mean and variance, To address this issue, several statistic-based sinogram restoration methods, such as the penalized weighted least square (PWLS) based and poisson likelihood (PL) based methods, have been proposed (Jing Wang *et. al.,* 2008; Liu Yan *et. al.,* 2012; Ma Jun, 2010). However, these existing methods often suffer from noticeable resolution loss especially in the case of constant noise variance over all sinogram data

(Gao, Yang *et. al.,* 2014).The formation of X-ray CT images can be modeled approximately by a discrete linear system as follows:

$$g = Af \qquad (5.1)$$

where $f = (f_1, f_2, ..., f_N)^T$, is the original image vector to be reconstructed, N is the number of voxels, the superscript T is the transpose operator, $g = (g_1, g_2, ..., g_M)^T$, is the measured projection vector data, M is the total number of sampling points in the projection data, $A = \{a_{ij}\}, i = 1, 2, ... M \; and \; j = 1, 2, ..., N$. is the system matrix, relating f and g, with the size $I \times J$, and its element a_{ij} is typically calculated as the intersection length of projection ray i with pixel j.

The line integral along an attenuation path is calculated according to the Lambert–Beer's law:

$$\tilde{g}_i = \ln\left(\frac{N_{0i}}{\tilde{N}_i}\right), \quad g_i \simeq \ln\left(\frac{N_{0i}}{N_i}\right) \qquad (5.2)$$

where N_{0i} represents the mean number of X-ray photons just before entering the patient and going toward the detector bin i, and can be measured by system calibration, e.g., by air scans; N_i denotes the detected photon counts at detector bin i with expected value $\tilde{N}_i$. The approximation for the second Eq. in (5.2) reflects an assumption that the Lambert–Beer's law can be applied to the random values (Zhang H *et. al.,* 2014).

Based on the previous studies, (Zhang H *et. al.,* 2014; Gao, Yang *et. al.,* 2014; Whiting Bruce *et. al.,* 2014; Zhang *et. al.,* 2010; Liu Li *et. al.,* 2012; Cui Xueying *et. al.,* 2014; Jing Wang *et. al.,* 2008'; Chen Y.*et. al.,* 2010) found that two principal sources of CT transmission data noise, X-ray quanta noise (signal–dependent compound Poisson distribution) and system electronic background noise (signal–independent Gaussian or normal distribution with zero mean). However, it is numerically difficult to directly implement these models for data noise simulation. Several reports have been discussed approximation of this model by the Poisson model (Srivastava Rajeev *et. al.,* 2013). Practically, the measured transmission data *I* can be assumed to statistically follow the Poisson

distribution upon a Gaussian distributed electronic background noise (Whiting Bruce *et. al.,* 2014):

$$N_i \approx Poisson\left(\tilde{N}_i\right) + Gaussian\left(m_e, \sigma_e^2\right) \tag{5.3}$$

where m_e and σ_e^2 are the mean and variance of the Gaussian distribution from the electronic background noise, $\tilde{N}_i$ is the mean of Poisson distribution.. In reality, the mean m_e of the electronic noise is often calibrated to be zero (i.e., 'dark current correction') and the associative variance slightly changes due to different settings of tube current, voltage and durations in a same CT scanner (Liu Li *et. al.,* 2012). Hence, in a single scan, the variance of electronic background noise can be considered as uniform distribution. Based on the noise model (5.3) and the use of the Lambert-Beer's law (5.2), the calibrated and log-transformed projection data follow approximately a Gaussian distribution with an associated relationship between the data sample mean and variance, which can be described by the following analytical formula (Niu Shanzhou *et. al.,* 2014):

$$\sigma_i^2 = \frac{1}{N_{0i}} \exp\left(\tilde{g}_i\right) \left(1 + \frac{1}{N_{0i}} \exp\left(\tilde{g}_i\right)\left(\sigma_e^2 - 1.25\right)\right) \tag{5.4}$$

where N_{0i} is the incident x-ray intensity, $\tilde{g}_i$ is the mean of the log transformed ideal sinogram datum g_i along path i, and σ_e^2 is the background Gaussian noise variance. In the implementation, the sample mean $\tilde{y}_i$ could be estimated by neighborhood averaging with a 3×3 window. The parameters N_{0i} and σ_e^2 can be measured as part of the standard routine calibration operation in modern CT systems (Zhang H *et. al.,* 2014).

According to previous studies (Yu, Lifeng *et. al.,* 2015; Zhang H *et. al.,* 2014; Gao Yang *et. al.,* 2014; Zhang *et. al.,* 2010; Liu Li *et. al.,* 2012; Cui Xueying *et. al.,* 2014; Jing Wang *et. al.,* 2008; Liu Yan et. al., 2012; Lui Dorothy et. al., 2013), the noisy line integral along an attenuated measurements can be treated as normally distributed with a non-linear signal-dependent variance (Liu Yan et. al., 2012; Lui Dorothy et. al., 2013). Assuming that the measurements among different bins are statistically independent, the likelihood function

of the joint probability distribution, given a distribution of the attenuation coefficients, can be written as:

$$P(g|f) = \frac{1}{Z_0} \prod_i \exp\left[-\frac{(g_i - f_i)^2}{2\sigma_i^2} \right] \tag{5.5}$$

where Z_0 is a normalizing constant, $g = (g_1, g_2, ..., g_M)^T$, is the is the measured projection vector data.

Then, ignoring the constant and irrelevant terms, and by taking the negative log-likelihood function can be written as:

$$L(g|f) = \ln P(g|f) = \sum_{i=1}^{M} \left\{ \frac{(g_i - f_i)^2}{2\sigma_i^2} \right\} \tag{5.6}$$

Due to the presence of an extremely limited number of X-ray projections, noise and other inconsistencies in the acquired sinogram data of CT image reconstruction causes an ill-posedness problem (Chen Y.*et. al.,* 2010). Therefore, the image estimation that directly optimizes the Maximum Likelihood (ML) criterion can be very noisy and unstable. So researchers reformulate this problem with the MAP estimation by posing a prior term to penalize or regularize the solution. The prior term enables us to incorporate available information or expected properties of the image to be reconstructed.

Mathematically, the MAP estimator can be expressed as:

$$f^* = \arg \max_f P(f|g) \tag{5.7}$$

According to the Bayesian law:

$$P(f|g) = \frac{P(g|f)P(f)}{P(g)} \tag{5.8}$$

By taking the logarithm and omitting the irrelevant term the MAP estimator can be simplified to:

$$f^* = \arg \max_f \left[\ln P(f|g) \right] = \arg \max_f \left[L(g|f) - R(f) \right] = \arg \max_f \left[L(g|f) - \lambda U(f) \right] \tag{5.9}$$

where *U(f)* denotes a penalty, and $\lambda > 0$ is a scalar control parameter which allows one to tune the MAP (or penalized ML (pML)) estimation for a specific noise-resolution tradeoff. When the value of λ goes to zero the reconstructed image from the MAP estimation approach behaves like the ML estimation.

The SIR of low-dose CT can be considered to estimate the attenuation map by maximizing the MAP (or pML) criterion with a non-negativity constraint (using the calibrated transmitted photon counts):

$$f^* = \arg\max_{f \geq 0} \left[L(g|f) - \lambda U(f) \right] \tag{5.10}$$

or directly minimizing the objective function by variational framework (using the calibrated line-integrals):

$$f^* = \arg\min_{f \geq 0} \left[\sum_{i=1}^{M} \frac{(g_i - f_i)^2}{2\sigma_i^2} + \lambda U(f) \right]$$

(5.11)

where $U(f)$ denotes the regularization term(e.g., the log-prior) and λ is the smoothing parameter that controls the trade-off between the data-fidelity term(e.g., the log-likelihood) and regularization term . In next section, we present the various possible choices available in literature for the regularization function or prior or penalty function $U(f)$.

5.2.1 Regularization strategies

The conceptual and mathematical model of regularization strategies will be illustrated explicitly in this section. Without loss of generality, we assume 2D configuration for the regularizations, while extension from 2D to 3D is straightforward (in 3D presentation, voxels would be used, instead of pixels). Here, image reconstruction problem can be cast into following minimization problem:

$$f^* = \arg\min_{f \geq 0} \left[L(g|f) + \lambda U(f) \right] \tag{5.12}$$

Let $U(f) = \frac{\lambda}{2} \langle Cf, f \rangle$,

$$= \arg\min_{f \geq 0} \left[\sum_{i=1}^{M} \frac{(g_i - f_i)^2}{2\sigma_i^2} + \frac{\lambda}{2} \langle Cf, f \rangle \right] \tag{5.13}$$

The first term $L(g|f) = \sum_{i=1}^{M} \frac{(g_i - f_i)^2}{2\sigma_i^2}$ measures the data fidelity for Gaussian noise and second term is a regularization function depending on the choice of C; λ is the regularization parameter that controls the degree of smoothing or regularization; and f^* is the obtained solution i.e. the processed or denoised image obtained by minimizing Eq. (5.13).

In this section, list of some possible choices of regularization function C are as follows:

1. If C= Square integral of the nth derivative of f: The penalized regularization function is known as a smoothing spline

2. If C=I_n *(Identity Matrix)*: The minimization problem given by Eq. (14) reduces to Tikhonov regularization which is in L2 framework and penalizes reconstructions with large L2-norm.

3. A common choice of Cf in CT/PET image reconstruction is the quadratic function written as :

$$Cf = \frac{1}{2} f^2 \tag{5.14}$$

A disadvantage of the quadratic prior (Zhang *et. al.,* 2010) is that it may oversmooth edges and small objects when a large value of λ is used in order to smooth out noise from large regions.

4. The second type of independent prior is based on the entropy function (Wang Guobao *et. al.,* 2011), whose corresponding energy function *(f)* can be described as:

$$Cf = \sum_{j} f_j \ln f_j \tag{5.15}$$

Basically, these two priors have the tendency to smooth both high-frequency edge regions and low-frequency background, so they cannot explicitly enforce smoothness in the image (Gui Z.g, 2013).

5. The third type of independent prior is the Gaussian prior (Zhang Quan et. al., 2013), whose energy function has the form:

$$Cf = \sum_j \frac{\left(f_j - \overline{f}_j\right)^2}{2\sigma_j^2} \qquad (5.16)$$

where x_j and σ_j^2 are the mean and variance respectively, and when $\overline{f}_j = 0$ it reduces to Eq. (5.16).

6. Similarly, the Gamma prior (Yuanquan Wang, 2008) allows only non-negative image values and can be a more natural model for an image:

$$Cf = \sum_j \rho\left(f_j, \overline{f}_j, \sigma_j\right) \qquad (5.17)$$

Where $\rho\left(f_j, \overline{f}_j, \sigma_j\right)$ is a Gamma PDF.

Basically, the Gaussian and Gamma priors encourage the neighbouring pixel values to be close to the mean image. Thus, the determination of the mean image has a significant effect on the reconstructed image (Yuanquan Wang, 2008). Some researchers investigated a new approach to estimate the mean image during the reconstruction using either the median or the mean of neighbouring pixels. However, in these cases, the priors are no longer truly independent.

7. The Tikhonov regularization is obtained by minimizing following:

$$f^* = \arg\min_{f \geq 0} \left\{ \sum_{i=1}^M \frac{\left(g_i - f_i\right)^2}{2\sigma_i^2} + \frac{\lambda}{2}|f|^2 \right\} \qquad (5.18)$$

8. If $Cf = \|\nabla f\|$: defined as Total Variation (TV), then L_1 norm of the second term in minimization problem given by Eq. (5.13) reduces to TV regularization (Zhang et. al., 2013). The TV penalized Gaussian maximum likelihood estimation is obtained by minimizing following Eq.:

$$f^* = \arg\min_{f \geq 0} \left\{ \sum_{i=1}^M \frac{\left(g_i - f_i\right)^2}{2\sigma_i^2} + \lambda|\nabla f| \right\} \qquad (5.19)$$

9. If $Cf = \nabla^2 f$: defined as Laplacian L_2 framework , the Laplacian penalized

Gaussian maximum likelihood estimation is obtained by minimizing following equation:

$$f^* = \arg\min_{f \geq 0}\left\{\sum_{i=1}^{M}\frac{(g_i - f_i)^2}{2\sigma_i^2} + \lambda|\nabla^2 f|\right\}$$ (5.20)

If $Cf = \|\nabla f\|^2$: defined as anisotropic diffusion in L$_2$ norm. Therefore, the second term in minimization problem given by Eq. (5.13) reduces to anisotropic diffusion regularization (Perona and Malik, 1990) which may also be converted to nonlinear complex diffusion (Srivastava Subodh *et. al.,* 2012) regularization after modification. The anisotropic diffusion penalized Gaussian maximum likelihood estimation is obtained by minimizing following:

$$f^* = \arg\min_{f \geq 0}\left\{\sum_{i=1}^{M}\frac{(g_i - f_i)^2}{2\sigma_i^2} + \frac{\lambda}{2}|\nabla f|^2\right\}$$ (5.21)

10. If $Cf = \|\nabla^2 f\|^2$: defined as Fourth order PDE. Afterwards, the second term in minimization problem given by Eq. (5.13) reduces to Fourth order PDE (Huaibin Wang et. al., 2012) regularization. The fourth order PDE penalized Gaussian maximum likelihood estimation is obtained by minimizing following:

$$f^* = \arg\min_{f \geq 0}\left\{\sum_{i=1}^{M}\frac{(g_i - f_i)^2}{2\sigma_i^2} + \frac{\lambda}{2}|\nabla^2 f|^2\right\}$$ (5.22)

Another form of priors assumes that the attenuation maps are locally smooth, i.e., the neighbouring pixels tend to have similar values.

11. One simple mathematical model that can describe this property is the Markov random field (MRF) model, also known as Gibbs distribution (Srivastava Subodh et. al., 2012) is defined as:

$$C(f) = \frac{1}{Z}\exp\left[-\lambda U(f)\right]$$ (5.23)

where Z is a normalizing constant.

12. Conventionally, the quadratic penalty value $U(f)$ is computed through a weighted sum of equal-distanced neighborhood pixels which is defined as :

$$U(f) = \sum_j \sum_{m \in W_j} w_{jm} \frac{1}{2} (f_j - f_m)^2 \qquad (5.24)$$

which corresponds to the Gaussian MRF (GMRF) prior (Zhang H et. al., 2014) that has been widely used for SIR. A major drawback of the GMRF prior is that it can excessively penalize the differences between neighbouring pixels when f_j and f_m fall across a discontinuous boundary in the image, thus may lead to over smoothing of edges and fine structures in the reconstructed image. To mitigate this issue, some researchers replaced the quadratic potential function with non-quadratic functions that increase less rapidly for sufficiently large differences. In this way, the corresponding priors are expected to remove noise while retaining sharp edges in the reconstructed image.

13. Another family of convex function prior is q-generalized Gaussian MRF prior (q-GGMRF) (Ma Jun, 2010), which can be described as:

$$C(\Delta) = \frac{|\Delta|^p}{1 + |\Delta/\delta|^{p-q}} \, (1 \leq q \leq p \leq 2) \qquad (5.25)$$

By giving specific parameter values, it can become:

$$C(\Delta) = \begin{cases} \Delta^2, (q = p = 2, Gaussian\ prior) \\ |\Delta|, (q = p = 1, median\ pixel\ prior) \\ |\Delta|^p, (1 < q = p \leq 2, generalized\ Gaussian\ MRF) \\ \dfrac{\Delta^2}{1 + |\Delta/\delta|}, (q = 1, p = 2, approximate\ Huber\ prior) \\ \dfrac{\Delta^p}{1 + |\Delta/\delta|^{p-q}}, (1 \leq q < p \leq 2, q - generalized\ Gaussian\ MRF) \end{cases} \qquad (5.26)$$

14. In Median root Prior (MRP), intensity differences among neighbouring pixels are not penalized. Instead, the penalty is set according to how much the central pixel differs from the local median. Mathematically, the MRP can be described as (Ma Jun, 2010):

$$U(f) = \sum_j \frac{(f_j - median(f_j))^2}{median(f_j)} \qquad (5.27)$$

where $median(f_j)$ is the local median. Therefore, no penalty is applied when the image is locally monotonic, and only non-monotonic local changes among neighbouring pixels are penalized. Although the MRP captures significant edges while encouraging preservation of locally monotonic regions, it is a heuristic empirical method and not convex in theory.

15. Recently, a new signal reconstruction theory, compressed sensing (CS) (Chun I Y and Talavage T M, 2013), has been rigorously formulated to accurately reconstruct a signal from much fewer samples than that is required by the Nyquist sampling theorem (Yuanquan Wang, 2008). The main idea of CS is that most signals are sparse in appropriate orthonormal systems, that is, a majority of their coefficients are close or equal to zero. Researchers tried to apply this theory to accurately reconstruct CT images at a much lower angular-sampling rate than the Nyquist sampling, but the CT images are generally not sparse in their original pixel representation (Srivastava R, 2010).

Mathematically, the CS method reconstructs an image via the L_p norm ($0 \leq p < 2$) minimization. Herein, for a vector f, $\| f \|_0$ represents the L_0 norm of vector f which counts the number of nonzero components of f, and $\| f \|_p$ ($p > 0$) denotes the L_p norm of vector f which is defined as:

$$\|f\|_p = \left(\sum_j |f_j|^p \right)^{1/p} \quad \rightarrow \quad \|f\|_p^p = \sum_j |f_j|^p \tag{5.28}$$

It should be noted that $\| f \|_p$ is not actually a norm when $0 \leq p < 1$ because it is not sub-additive, yet we still refer it as norm following convention (sort of abuse of terminology).

16. The next choice is total-variation (TV) which is widely used penalty function in image reconstruction that avoids smoothing of salient details (Ghita, O et. al., 2010), which is given as the 1-norm of the gradient of the solution. Regularization with the TV penalty results in smoothing of weakly varying details and preservation of salient (having strong variation) details such as edges:

$$C(f) = \sqrt{f + T^2} - T \qquad (5.29)$$

where, T is a thresholding parameter. Another methods to reduce the amount of noise present in the images, we used a high performance spatially adaptive

17. Block matching 3D filter (BM3D), (Wang G. et. al., 2012) which is used for the noise removal. BM3D is based on the assumption that a noise-free image spectrum of similar image fragments group can be better approximated as a combination of a few spectrum elements than a single image fragment (Wang G. *et. al.,* 2012). Afterwards, a patch-based regularization proposed by (Wang G. *et. al.,* 2012).

18. Traditional regularizations penalize image roughness based on the intensity difference between neighbouring pixels, but the pixel intensity differences may not be reliable in differentiating sharp edges from random fluctuation due to noise. To address this issue, Probabilistic Patch-Based (PPB) regularizations proposed by (Wang G. *et. al.,* 2012) which utilize neighborhood patches instead of individual pixels to measure the image roughness. Since they compare the similarity between patches, the patch-based regularizations are believed to be more robust in distinguishing real edges from noisy fluctuation. The patch-based roughness regularizations are defined as:

$$U(f) = \sum_{j=1}^{n_j} \sum_{k \in SW_j} w_{jk} C\left(\left\| f_j(x) - f_k(x) \right\|_{2,c} \right) \qquad (5.30)$$

where $w_{jk} = 1$, or $w_{jk} = 1/d_{jk}$ and $f_j(x)$ and $f_k(x)$ is the feature vector consisting of intensity values of all pixels in the patch centred at pixel j and k respectively.

A wide variety of regularization methods has been discussed in this section such as the quadratic membrane (QM) (Zhang Quan et. al., 2013) prior, Gibbs prior (Gui Z.g, 2013), entropy prior (Srivastava R, 2010), Huber prior function (Yang Chen, 2008), total variation (TV) prior (17], and some edge-preserving priors. These priors were able to preserve sharp edge information by choosing a non-quadratic prior (Wang G. et. al., 2012; Wang Guobao et. al., 2011; Ma Jun, 2010; Rajeev Srivastava, 2010; Srivastava R, 2010). However, in the case of low X-ray scan where the noise level is relatively significant, such edge-preserving quadratic and non-quadratic priors tend to produce blocky piecewise regions or staircase artifacts. None of these priors ad-

dresses the information of global connectivity and continuity in objective image. Only local and in discriminatively prior information is provided. Thus, to address these drawbacks in the existing priors, here we proposed a new variational framework for sinogram restoration in case of low-dose X-ray CT reconstruction in the next section.

5.3 The Proposed variational framework for sinogram restoration

In this section, we present a new variational model of sinogram restoration based on the choice of proposed regularization function. The proposed prior is an extension of nonlinear AD based filter. It uses the concept of Convex virtual field (abbreviated as: CONVEF) to deal with case of mixed noise in the sinogram data. In addition to denoising signal dependent Gaussian noise the sinogram data may also contain some other additive noise such as quantum or background noise which we can defined as signal independent Gaussian noise. For simplicity, we can say that low-dose sinogram data are corrupted with mixed type noise i.e. signal dependent and signal independent Gaussian noise. Therefore, the proposed regularization term is well capable of handling such type of noise effectively and efficiently.

In this work, we incorporate a novel CONVEF based P-M anisotropic diffusion term into an energy function for statistical sinogram smoothing. The energy minimization function is used to obtain sinogram smoothing. In variational framework (Ghita, O et. al., 2010), the minimization problem given by Eq. (5.13) can also be defined as:

$$f^* = \arg\min_{f \geq 0} E(f) \tag{5.31}$$

where the energy functional is described as follows:

$$E(f) = E_1(f) + \lambda E_2(f) \tag{5.32}$$

In Eq. (5.32), $E_1(f)$ is known as a data fidelity term or data energy, which ensures the consistency between the ideal projection data f and the measurement g.

$E_2(f)$ is a regularization term or smoothness energy. The parameter λ is introduced to control the degree of agreement between the estimated and the measured data.

In the MRF framework, the data energy comes from ignoring the constant and irrelevant terms and by taking the (negative) log-likelihood function of the observed projection data (Chen Y.et. al., 2010).According to the noise model, the joint probability distribution of the projection data which can also be expressed in Eq. (5.33) as:

$$P(g|f) = \prod_{i=1}^{M} P(g_i|f_i) = \prod_{i=1}^{M} \frac{1}{\sqrt{2\pi\sigma_i^2}} \exp\left(-\frac{(g_i - f_i)^2}{2\sigma_i^2}\right) \qquad (5.33)$$

where $g = (g_1, g_2, ..., g_M)^T$, is the measured projection vector data. Then, ignoring the constant and irrelevant terms, the negative logarithm function can be written as:

$$E_1(f) = \ln P(g|f) = \sum_{i=1}^{M} \left\{ \frac{(g_i - f_i)^2}{2\sigma_i^2} \right\} \qquad (5.34)$$

In the MRF framework, the smoothness energy comes from the negative log likelihood of the *priori* (Zhang et. al., 2010). In this work, we choose nonlinear CONVEF based P-M anisotropic diffusion regularization term for two reasons. One is that, due to the integral nature of the edge-preserving MRF priori, does not suit well for high continuity of the projection data. Another is that the smoothness energy $E_2(f)$ has a quadratic form (thus convex) and a prior model like CONVEF based P-M anisotropic diffusion permits an optimal solution of Eq. (5.31) in a computationally acceptable time. With MRF, the smoothness energy has the form as:

$$E_2(f) = \arg\min\left(\lambda \int_{\Omega} \phi\left(\|\nabla f\|^2\right) d\Omega\right) \qquad (5.35)$$

where $\phi(\|\nabla f\|^2)$ is defined as gradient norm of image corresponding energy function. The solution of the proposed sinogram smoothing of Eq. (5.32) can be described by substituting Eq. (5.34) and (5.35) to Eq. (5.32), we get:

$$E(f) = \underset{f \geq 0}{\arg\min}\, E(f) = \sum_{i=1}^{M} \left\{ \frac{(g_i - f_i)^2}{2\sigma_{y_i}^2} \right\} + \int_{\Omega} \left(\lambda \|\nabla f\|^2 \right) d\Omega \qquad (5.36)$$

The functional $E(f)$ is defined on the set of $f \in BV(\Omega)$ such that $\log f \in L^1(\Omega)$ and f must be positive everywhere. After minimizing Eq. (5.36) using Euler–Lagrange minimization technique combined with gradient descent approach, the solution to above Eq. (5.36) can be written as:

$$f_t = \frac{(g_i - f_i)}{\sigma_i^2} + \lambda\, div\left(c\left(|\nabla f| \right) \nabla f \right), \quad with \quad \frac{\partial f}{\partial \vec{n}} = 0 \; on \; \partial\Omega \qquad (5.37)$$

where div is the divergence operator and ∇ is the gradient operator, $f_{(t=0)} = f_0$ is the initial condition for noisy image. The diffusion coefficient $c(\cdot)$ is a nonnegative function of the image gradient. Generally $c(\cdot)$ takes as:

$$c_1\left(|\nabla f| \right) = \exp\left(-\left(|\nabla f|/k \right)^2 \right) \quad and \quad c_2\left(|\nabla f| \right) = 1/1 + \left(\left(|\nabla f|/k \right)^2 \right) \quad (5.38)$$

where k is a conductance parameter also known as gradient magnitude threshold parameter that controls the rate of diffusion and the level of contrast at the boundaries. Since the scale-space generated by these two functions is different. The diffusion coefficients, c_1 favours high contrast edges over low-contrast ones while c_2 favours wide regions over small ones. Moreover, when the value of k is a small, weak edges will be preserved but the denoising capability is weak. Conversely, the denoising capability is strong but weak edges and fine details will be smoothed as well when k is a large value.

From the literature (Perona and Malik, 1990; Hongchuan yu, 2004; Yuanquan Wang, 2008; Zhang Quan et. al., 2013; Gui Z.g, 2013; Buyle P et. al., 2007; Srivastava R, 2010), it is well known that in nonlinear AD prior diffusion is controlled by a variable coefficient in order to preserve edges. This prior is typically used as a feature-preserving denoising algorithm. However, P-M diffusion model can remove isolated noise and preserve the edges up to some extent. But, it cannot preserve the edge details effectively and accurately, therefore tends to cause blocking staircase effect. Its performance is worst for very noisy images. It's smooth of an image near pixels with a large gradient magnitude

(i.e., at the edge pixels). Thus, noise at edges cannot be removed by permitting more diffusion along the edge than across it. To address these limitations of AD method as prior, here the CONVEF based P-M anisotropic diffusion process is introduced as a second term in the above mentioned (in Eq. 5.37) regularization framework. The expanded form of the second term i.e. AD based prior (Yuanquan Wang et. al., 2010), which is defined as:

$$div\left(c'\left(|\nabla f|\right)\nabla|\nabla f|\cdot\nabla f + c\left(\nabla f\right)\nabla^2 f\right) \tag{5.39}$$

where,

$c'\left(|\nabla f|\right)\nabla|\nabla f|\cdot\nabla f$ An inverse diffusion term used for enhance or sharpen the boundaries,

$c\left(\nabla f\right)\nabla^2 f$ Laplacian term used for smoothing the regions that are relatively flat,

∇f A term used to displace the inverse diffusion term to improve the denoising effect, as the GVF field basically implements a weighted gradient diffusion process.

Since, the GVF-based P–M Eq. is vulnerable when the image data is corrupted by both poisson and Gaussian noises. As a solution to this, an Inverse GVF (INGVF) based P–M model (Ghita, O et. al., 2010), which shows more stability in the presence of poisson and Gaussian noises, was developed. However, both the GVF and INGVF need a complicated computation process and their noise robustness is not always guaranteed. To deal with this issue while still preserving strong and weak edges, here the inverse diffusion term based on CONVEF AD is redesigned to improve the P–M equation. The CONVEF is equivalent to gradient diffusion, just like the GVF and INGVF, but it performs better than these two fields. Thus, we have used here a CONVEF-based P–M Eq. defined as:

$$f_t = \left(1 - IN\left(f_0\right)\right)\left(med\left(f_0\right) - f_{t-1}\right) + IN\left(f_0\right)\cdot\left(-\mathrm{E}_{\mathrm{CONVEF}}\cdot\nabla f + c\nabla^2 f\right) \tag{5.40}$$

where f_0 is the input noisy image, f_{t-1} is the updated f at iteration $t-1$. IN (f_0) is the signal dependent and signal independent Gaussian estimator defined

in (Baodong Liu., 2011), *med* is the median filter and E_{CONVEF} denotes the Convolutional Virtual Electric Field defined as follows (Ghita, O *et. al.,* 2010):

$$E_{CONVEF} = \left(-\frac{a}{r_h^{n+2}} \otimes q, -\frac{b}{r_h^{n+2}} \otimes q \right) \tag{5.41}$$

where,

$r_h = \sqrt{a^2 + b^2 + h}$ An effective kernel that modifies the distance metrics,

h   The factor which plays a role analogous to scale space filtering,

a and b   Virtual electric field in the image pixel, and

q   Magnitude of the image edge maps.

The larger the value of *h*, greater is the smoothing effects on the results; on the other hand, the larger the value of *n*, faster is the potential decay with distance and vice versa. These properties allow the CONVEF snakes to preserve edges and to tell apart two closely-neighbored objects with large *n* and to enter into C-shaped concavities with small *n*.

In Eq. (5.39), second order derivative of P-M Eq. is computed. To solve this complexity of deriving second derivative Eq. (5.40), in which E is determined before image evolution and only ∇f needs to be computed directly from the observed image in the inverse diffusion term, is proposed. The proposed model have advantages of both GVF and INGVF-based P–M equation, such as robust estimation of high-order derivative and numerical stability improvement.

Therefore, the proposed model Eq. (5.39) will benefit from the computational cost and it may effectively remove mixed noise i.e. signal dependent and signal independent present in low dose sinogram data. The above discussed model in Eq. (5.40) could be broken in two parts according to the type of noise properties. For example, if the pixels in image are corrupted by impulse or electronic noise (IN $\approx$ 0), then the output of the image enhancement process shown in Eq. (5.40)

approximates the output of the median filter, and the discrete implementation of Eq. (5.40) becomes

$$f_t = f_{t-1} + d_t \left(med\left(f_0 \right) - f_{t-1} \right) \tag{5.42}$$

where d_t denotes the time step. If the pixels in image are corrupted by Gaussian noise (IN $\approx$ 1), then the discrete implementation of Eq. (5.40) equivalent to:

$$f_t = f_{t-1} + d_t \cdot f_t = f_{t-1} - d_t \left(E_{CONVEF} \cdot \nabla f_{t-1} + c\nabla^2 f_{t-1} \right). \tag{5.43}$$

After introducing the concepts of above mentioned CONVEF-AD based approach adapted to mixed noise reads as:

$$\frac{\partial f}{\partial t} = \frac{\left(g_i - f_i \right)}{\sigma_i^2} + \lambda\left(c'\left(\left| \nabla f \right| \right) \nabla \left| \nabla f \right| \cdot \nabla f + c\left(f \right) \nabla^2 f \right), \quad with \quad \frac{\partial x}{\partial \vec{n}} = 0 \; on \; \partial\Omega \tag{5.44}$$

This model is capable of dealing with the case of mixed noise sinogram data. Now applying the solution of CONVEF AD using Eq. (5.44). The proposed model in Eq. (5.39) can be re-written as follows:

$$\frac{\partial f}{\partial t} = \frac{\left(g_i - f_i \right)}{\sigma_i^2} + \lambda\left(\left(1 - IN\left(f_0 \right) \right)\left(med\left(f_0 \right) - f_{t-1} \right) + IN\left(f_0 \right) \cdot \left(-E \cdot \nabla f + c\nabla^2 f \right) \right), \tag{5.45}$$

where IN $\approx$ 0, for image are corrupted by impulse or electronic noise and IN $\approx$ 1, for image are corrupted by signal dependent Gaussian noise. The value of k is set to σ_e which is minimum absolute deviation (MAD) of the gradient of an image. The adaptive value of k is estimated as:

$$k = \sigma_e = 1.4826 \times median_f \left[\left\| \nabla f - median_f \left(\left\| \nabla f \right\| \right) \right\| \right] \tag{5.46}$$

Using gradient descent to solve Eq. (5.45), the solution is obtained by

$$f_t^n = \frac{\left(g_i^n - f_i^n \right)}{\left(\sigma_i^2 \right)^n} + \lambda\left(\left(1 - IN\left(f_0 \right) \right)\left(med\left(f_0 \right) - f_{t-1}^n \right) + IN\left(f_0 \right) \cdot \left(-E^n \cdot \nabla f^n + c\nabla^2 f^n \right) \right),$$

$$\tag{5.47}$$

where the index n represents the iterative number. For digital implementations, the Eq. (5.47) can be discretized using finite differences schemes (Srivastava Rajeev *et. al.,* 2013). After discretization of the proposed modified CONVEF AD model, given by Eq. (5.47), reads

$$\frac{f_{i,j}^{n+1} - f_{i,j}^{n}}{\Delta t} = \frac{\left(g_{i,j}^{n} - f_{i,j}^{n}\right)}{\left(\sigma_{i,j}^{2}\right)^{n}} + \lambda\left(\left(1 - IN\left(f_{0}\right)\right)\left(med\left(f_{0}\right) - f_{t-1}^{n}\right) + IN\left(f_{0}\right)\cdot\left(-E^{n}\cdot\nabla f^{n} + c\nabla^{2}f^{n}\right)\right),$$

(5.48)

$$f_{i,j}^{n+1} = f_{i,j}^{n} + \Delta t\left[\frac{\left(g_{i,j}^{n} - f_{i,j}^{n}\right)}{\left(\sigma_{i,j}^{2}\right)^{n}} + \lambda\left(\left(1 - IN\left(f_{0}\right)\right)\left(med\left(f_{0}\right) - f_{t-1}^{n}\right) + IN\left(f_{0}\right)\cdot\left(-E^{n}\cdot\nabla f^{n} + c\nabla^{2}f^{n}\right)\right)\right],$$

(5.49)

For the discretized versions of Eq. (5.48) & (5.49) to be stable, the von Neumann analysis (Srivastava Rajeev *et. al.,* 2013) shows that we require $\Delta t/(\Delta f)^{2} < \frac{1}{4}$. If the grid size is set to $\Delta f = 1$, then the value of Δt is set to $\Delta t \leq 1/4$. Therefore, the value of Δt is set to $1/4$ for stability of Eq. (5.49).

Proposed Algorithms:

The Pseudo code for the proposed framework can be summarized as:

CONVEF-AD based Sinogram Restoration Step

1. Initialize: $g_{0}, N_{0}, \sigma_{e}^{2}, \lambda; Niter = 20;$;

2. for $j=1,2,....,N$ (Data variance estimation)

3. g_{j} = measured projection data

4. $\hat{g}_{i} = \sum_{j \in N_{i}^{3\times3}} g_{j}/9$; (Mean of projection data over 3×3 window)

5. $\sigma_{i}^{2} = \frac{1}{N_{0i}}\exp\left(\tilde{g}_{i}\right)\left(1 + \frac{1}{N_{0i}}\exp\left(\tilde{g}_{i}\right)\left(\sigma_{e}^{2} - 1.25\right)\right)$;

6. end for

7. Calculate the gradient coefficient:

$$c\left(\left|\nabla f\right|\right) = \omega\exp\left(-\left(\frac{\left|\nabla f\right|}{K}\right)^{2}\right)$$

where $\omega_{jm} = \dfrac{\exp\left(-\left\|f(n_j) - f(n_m)\right\|_E^2 / h^2\right)}{d_{jm}}$

8. Calculate the gradient magnitude threshold:

9. $k = \sigma_e = 1.4826 \times median_f\left[\left\|\nabla f - median_f\left(\|\nabla f\|\right)\right\|\right]$

10. Initialize: $a, b, q, h, r_0\ n$;

11. while (stop criteria is not met)

12. Calculate: $E_{CONVEF} = \left(-\dfrac{a}{r_h^{n+2}} \otimes q, -\dfrac{b}{r_h^{n+2}} \otimes q\right)$;

13. For $l = 1, 2, \ldots, L$; (AD Gradient Descent)

14. $f_{i,j}^{n+1} = f_{i,j}^n + \Delta t\left[\dfrac{\left(g_{i,j}^n - f_{i,j}^n\right)}{\left(\sigma_{i,j}^2\right)^n} + \lambda\left(\left(1 - IN(f_0)\right)\left(med(f_0) - f_{i-1}^n\right) + IN(f_0)\cdot\left(-E^n\cdot\nabla f^n + c\nabla^2 f^n\right)\right)\right]$;

15. update:

$c'(|\nabla f|) = \omega\exp\left(-\left(\dfrac{|\nabla f|}{K}\right)^2\right)$

16. update:

17. $\sigma_i^2 = \dfrac{1}{N_{0i}}\exp(\tilde{g}_i)\left(1 + \dfrac{1}{N_{0i}}\exp(\tilde{g}_i)\left(\sigma_e^2 - 1.25\right)\right)$

18. end for;

19. End if stop criteria is satisfied.

20. Repeat Steps A and B until Eq. (5.49) converges to a relative stable solution.

21. Reconstruct the object image using FBP from the smoothed sinogram obtained from step 20.

5.4 Results and Discussions

In this work, two test cases are used shown in Fig. 5.1, both are computer generated mathematical simulated modified Shepp-Logan head phantom and hot and cold phantom utilized to validate the performance of the proposed CONVEF-AD based sinogram smoothing method for low-dose CT reconstruction. For simulation study MATLAB 2013b software was used on a PC with Intel(R) Core (TM) 2 Duo CPU U9600 @ 1.6GHz, 4.00 GB RAM, and 64 bit MS window operating system. The brief description of the various parameters used for

generation and reconstruction of the two test cases are as follows: Both test cases are of size 128 x128 pixels and 120 projection angles were used. To simulate the noisy low-dose sinogram data, Eq. (5.3) was used, which is in mixed noise nature i.e. Both signal dependent and signal independent Gaussian distributed and all assumed to be 128 radial bins and 128 angular views evenly spaced over 1800. A mixed noise of magnitude 10% is added to sinogram data. In simulation purposes fan-beam imaging geometry were used. By applying radon transform noise free sinogram were generated which is shown in Fig. 5.2(b) and 5.3(b). After that isolated data from the noisy sinogram which are shown in Fig. 5.2(c) and 5.3(c), were extracted by applying a 3x3 median filter and select the output as an initial estimator. Also compute the mean and variance by using Eq. (5.4) and then calculate the gradient coefficient by applying Eq. (5.38). The value of conductivity coefficient k (kappa) was set to 0.033 to 1.0 for different test cases and within each MLEM step, AD is run for 3 iterations.

The value of was set to 0.24 and the value of diffusion coefficient (Kappa) used by proposed CONVEF-AD based prior was set to 0.033 to 1.0 for different test cases, within each iteration during sinogram smoothing. Update the value of estimation pixel by pixel using Eq. (5.18) until not reaches to a relative convergence. The reconstructed images generated by different algorithms are shown in Fig.5.2 (d, e, f) & 5.3(d, e, f) respectively. From the figures, we can see that the proposed algorithm has well performance of noise removal and edges preservation especially the thin edges and detail information. At the same time, we can observe that the CONVEF-AD algorithm overcomes the shortcoming of streak artifacts and the reconstructed image is more similar to the original phantom. In our study, the suitable value for iteration number N is 15 because visual result hardly changes for further iterations. The graphs are plotted for SNR, RMSE, CP, and MSSIM along with number of iterations for different algorithms are shown in Fig. 5.4-5.7, for two different test cases. From Fig. 5.4, it is observed that the SNR, values associated with the proposed method is always higher than that produced by other algorithms such as Total variation (TV) and Anisotropic Diffusion (AD) priors with traditional Filtered Back-projection (FBP), which indicates that the CONVEF-AD with FBP framework significantly improves the quality of reconstruction in terms of SNR, RMSE, CP, and MSSIM values. Fig-

ure 5.5 shows that the RMSE values of proposed method are higher in comparison to other methods which indicate that the proposed method is performing better. Figure 5.6 shows that the CP values of proposed method are higher and close to unity in comparison to other methods which indicate that the proposed method is also capable of preserving the fine edges and structures during the reconstruction process. Figure 5.7, shows that the MSSIM values of proposed method is higher which indicate that better reconstruction; it also preserves the luminance, contrast and other details of the image during the reconstruction processes.


Fig 5.1: The phantoms used in the simulation study, Modified Shepp-Logan phantom (128 x 128 pixels), CT Test phantom (128 x 128 pixels)

(a)   (b)   (c)

(d)   (e)   (f)
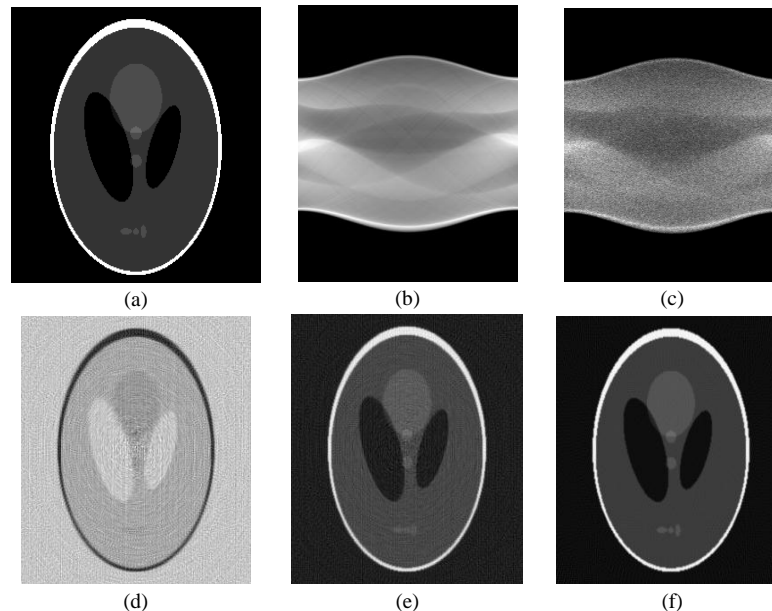
Fig 5.2: The Modified Shepp-Logan phantom with different reconstruction methods from the noise-free and noisy data.Original Shepp-Logan phantom, (b) noise free sinogram (c) noisy sinogram (d) reconstructed image by TV+FBP, (e) reconstructed result by AD+FBP, (f) reconstructed result by CONVEF_AD+FBP
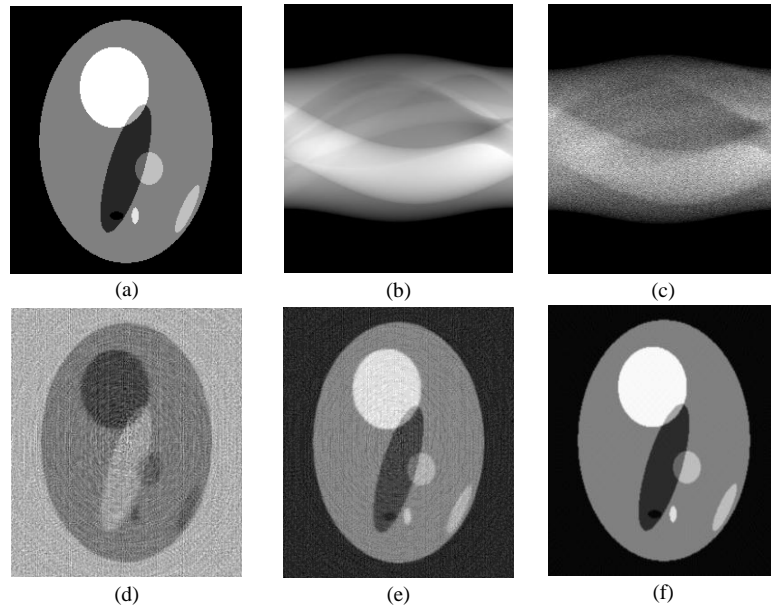
Fig 5.3: The CT phantom with different reconstruction methods from the noise-free and noisy data. Original Shepp-Logan phantom, (b) noise free sinogram (c) noisy sinogram (d) reconstructed image by TV+FBP, (e) reconstructed result by AD+FBP, (f) reconstructed result by CONVEF_AD+FBP
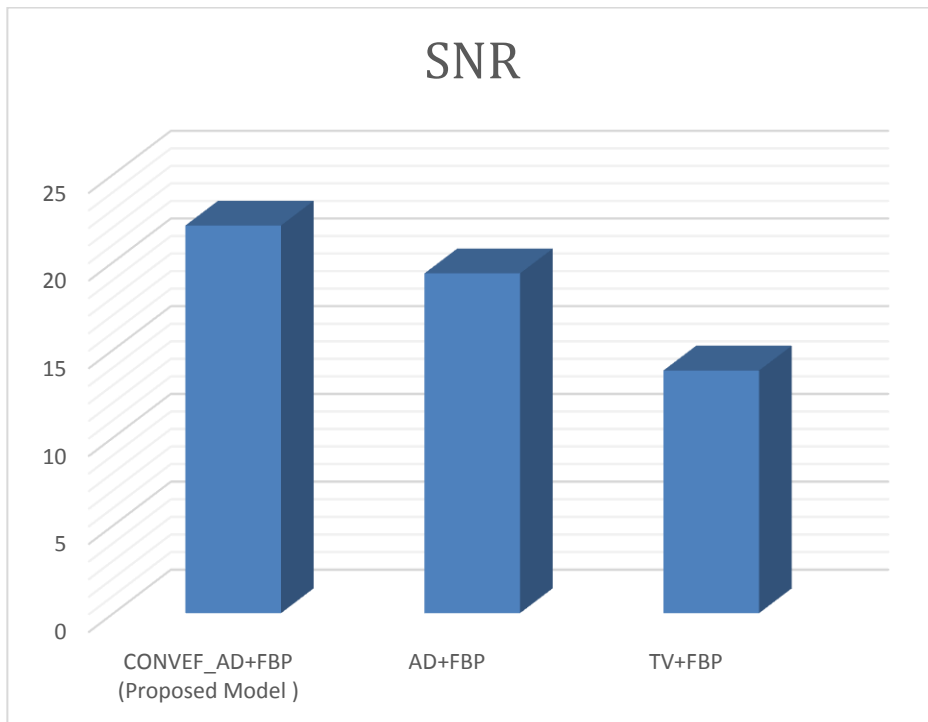
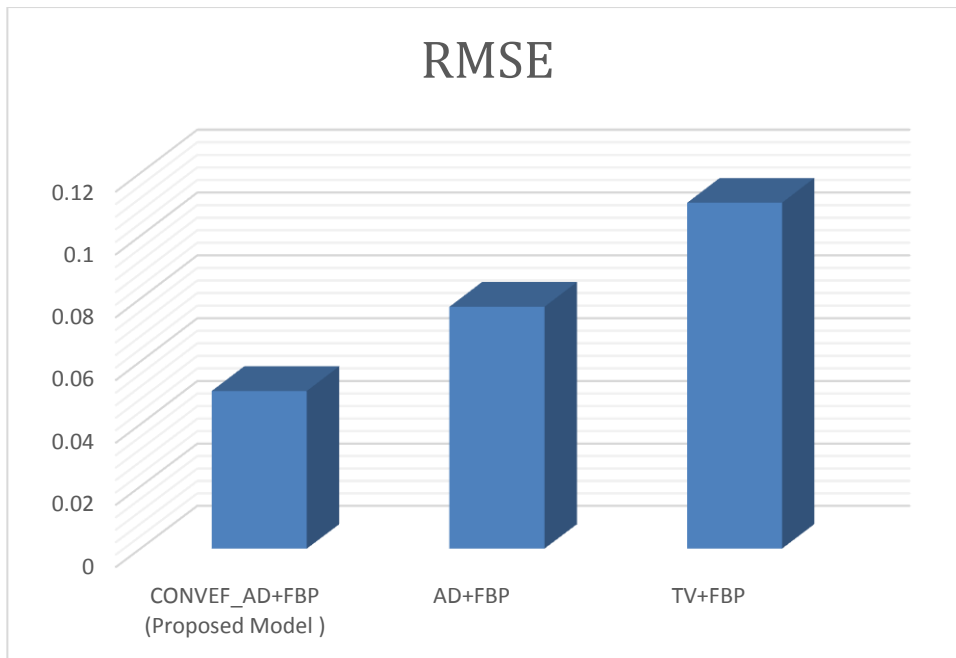Fig. 5.4: The Plots of SNR along with No. of Iterations for different reconstruction algorithms for Test case 1

Fig. 5.5: The Plots of RMSE along with No. of Iterations for different reconstruction algorithms for Test case 1
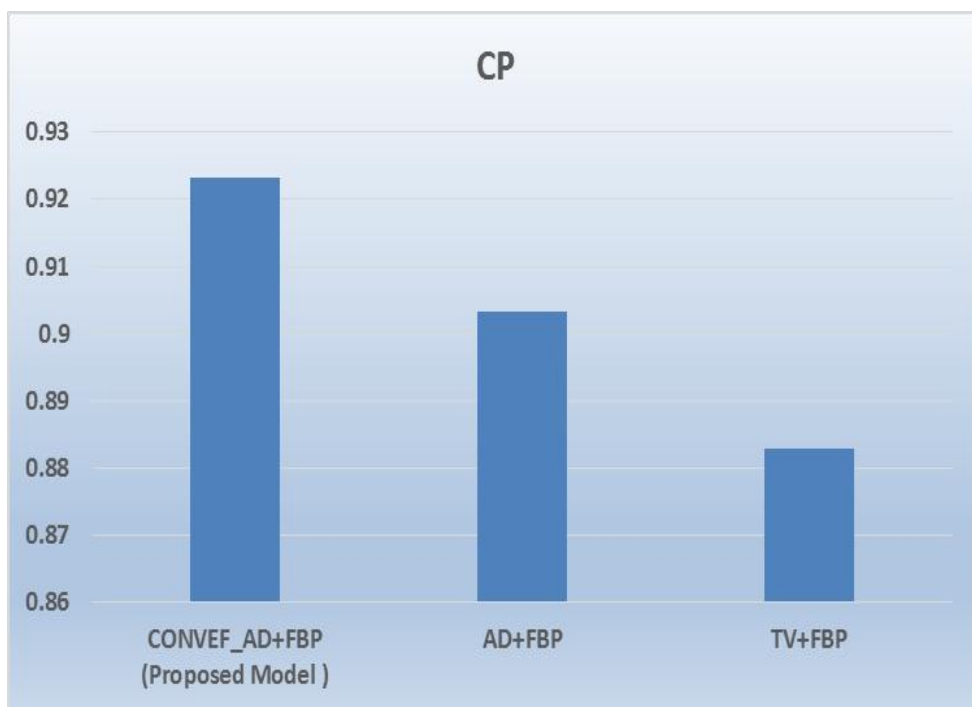

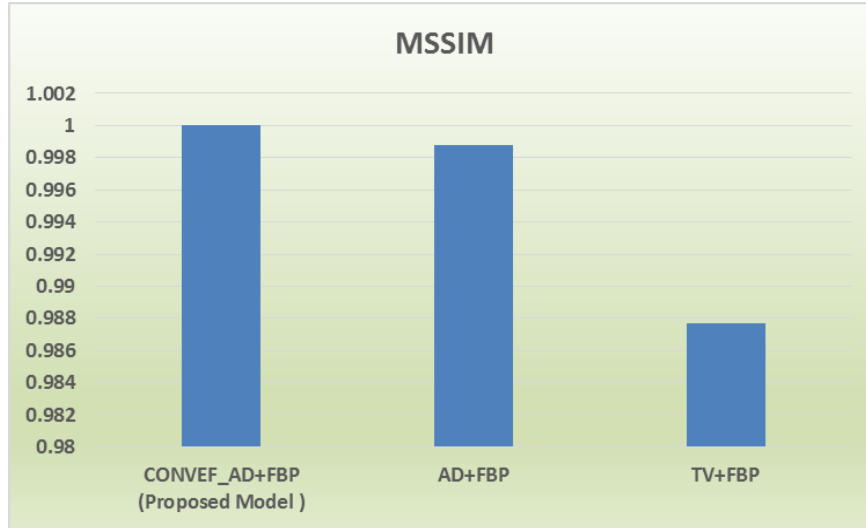Fig. 5.6: The Plots of CP along with No. of Iterations for different reconstruction algorithms for Test case 1

Fig. 5.7: The Plots of MSSIM along with No. of Iterations for different reconstruction algorithms for Test case 1

5.5 Conclusion

In this work, proposed an efficient method for statistical sinogram smoothing for low-dose X-ray CT reconstruction. The proposed method is modelled into a variational framework. The solution of the method, based on minimization of an energy functional, which consists of two terms viz. data fidelity term and a regularization function. The data fidelity term was obtained by minimizing the negative log likelihood of the signal dependent Gaussian probability distribution, which depicts the noise distribution in low dose X-ray CT. The second term i.e. regularization term was a non-linear CONVEF-AD (CONvolutional Virtual Electric Field Anisotropic Diffusion) based filter, an extension of Perona–Malik (P–M) anisotropic diffusion filter. The role of regularization function was to resolve the ill-posedness of first term. The proposed method was capable of dealing with both signal dependent and signal independent Gaussian noise i.e. mixed noise. For experimental purpose, two different sinograms generated from test phantom images are used. The comparative study and performance evaluation of the proposed method with other standard methods is also presented. The obtained results indicate that the proposed method possess better mixed noise removal capability than other methods in low dose X-ray CT.